

UC Davis

UC Davis Previously Published Works

Title

Production of recombinant human tektin 1, 2, and 4 and in vitro assembly of human tektin 1

Permalink

<https://escholarship.org/uc/item/2fh5b0m4>

Journal

Cytoskeleton, 75(1)

ISSN

1949-3584

Authors

Budamagunta, MS

Guo, F

Sun, N

et al.

Publication Date

2018

DOI

10.1002/cm.21418

Peer reviewed



Published in final edited form as:

Cytoskeleton (Hoboken). 2018 January ; 75(1): 3–11. doi:10.1002/cm.21418.

Production of recombinant human tektin 1, 2, and 4 and in vitro assembly of human tektin 1

MS Budamagunta¹, F. Guo², N Sun³, B Shibata³, PG FitzGerald³, JV Voss¹, and JF Hess³

¹Department of Biochemistry and Molecular Medicine, University of California, DAVIS, CA, 95616

²Department of Molecular and Cellular Biology, University of California, DAVIS, CA, 95616

³Department of Cell Biology and Human Anatomy, University of California, DAVIS, CA, 95616

Abstract

Proteins predicted to be composed of large stretches of coiled-coil structure have often proven difficult to crystallize for structural determination. We have successfully applied EPR spectroscopic techniques to the study of the structure and assembly of full-length human vimentin assembled into native 11 nm filaments, in physiologic solution, circumventing the limitations of crystallizing shorter peptide sequences. Tektins are a small family of highly alpha helical filamentous proteins found in the doublet microtubules of cilia and related structures. Tektins exhibit several similarities to IFs: moderate molecular weight, highly alpha helical, hypothesized to be coiled-coil, and homo- and heteromeric assembly into long smooth filaments. In this report, we show the application of IF research methodologies to the study of tektin structure and assembly. To begin *in vitro* studies, expression constructs for human tektins 1, 2 and 4 were synthesized. Recombinant tektins were produced in *E. coli* and purified by chromatography. Preparations of tektin 1 successfully formed filaments. The recombinant human tektin 1 was used to produce antibodies which recognized an antigen in mouse testes, most likely present in sperm flagella. Finally, we report the creation of 7 mutants to analyze predictions of coiled-coil structure in the rod 1A domain of tektin 1. Although this region is predicted to be coiled-coil, our EPR analysis does not reflect the parallel, in register, coiled-coil structure as demonstrated in vimentin and kinesin. These results document that tektin can be successfully expressed and assembled in vitro, and that SDSL EPR techniques can be used for structural analysis.

Introduction

Tektins are a family of structural proteins found in cilia and related structures [Amos 2008; Linck et al. 2016] [Yanagisawa and Kamiya 2004]. When originally identified, antibody reactivity and protein sequences of tektin isoforms suggested an evolutionary relationship to intermediate filaments [Chang and Piperno 1987; Chen et al. 1993; Norrander et al. 1992]. Protein structure predictions suggest that tektins are highly alpha helical, coiled-coil proteins that assemble into rod shaped filaments, thus structurally resembling IFs [Linck et al. 2014; Norrander et al. 1996]. Tektins have been most well characterized in sea urchin flagella using an elegant step-wise disassembly protocol which reveals the long, straight, uniform

The authors declare no conflicts of interest.

looking filament localized to protofilaments A11-12-13-1 of the flagellar doublet microtubule [Linck et al. 2014]. The predicted coiled-coil structure, association of tektin at specific protofilaments and the evidence of sperm motility defects in mice with tektin mutations [Roy et al. 2007; Roy et al. 2009] [Tanaka et al. 2004] [Yanagisawa and Kamiya 2004] all support the hypothesis that tektins are structural proteins that provide reinforcement of the doublet microtubule and thus, the flagellum.

The description of alpha helical coiled-coil structure was deduced by Crick and described as the packing of knobs into holes [Crick 1953]. A key component of the structure described by Crick is that non-polar residues should be located approximately every 3.5 residues. When amino acid sequences for KMEF (keratin, myosin, epidermin, fibrinogen) proteins became widely available, the heptad repeat nature (*a-b-c-d-e-f-g*) coupled with the prevalence of nonpolar amino acids at *a* and *d* positions confirmed Crick's hypothesis. The support for the hypothesis is such that coiled-coil structure is almost universally predicted wherever a nonpolar *a,d* heptad repeat pattern is found. Only more recently has the phenomena of long single alpha helices been recognized as an alternative to coiled-coils in myosin 10 and the inner centromere protein (INCENP) [Knight et al. 2005; Samejima et al. 2015; Suveges et al. 2009].

Short coiled-coil domains within globular proteins, often mediating dimerization, have been solved by crystallization [O'Shea et al. 1991; Saudek et al. 1991; Ellenberger et al. 1992; Konig and Richmond 1993]. However, elongated coiled-coil domains frequently predicted in fibrous proteins such as Intermediate Filaments (IFs), myosins, and tektins are generally resistant to crystallization. Recent analyses of full length IF proteins by electron paramagnetic resonance spectroscopy of site-directed spin labels (SDSL-EPR) has resulted in considerable advances in the determination of the structure of the vimentin central rod domain. Spectroscopic data provided the first data supporting coiled-coil structure in rod 1B and 2B of full length human vimentin [Hess et al. 2004; Hess et al. 2002]. However, despite long standing predictions, EPR data also showed that vimentin linker 2 was a rapidly assembling, very stable, parallel dimer of protein chains and not a coiled-coil [Hess et al. 2006]. At nearly the same time a hypothesis was advanced to describe the hendecad repeat structure of vimentin rod 2A and linker 2 regions as "adopting a continuous right-handed coiled-coil structure with a long-period pitch length" (long period pitch equivalent to parallel helices) [Parry 2006]. Several years later, the structure of a peptide containing rod 2A, linker 2 and the beginning of rod 2B sequences was solved by x-ray crystallography [Nicolet et al. 2010]. The crystal was a symmetric assembly of 4 peptides revealing both parallel helices and coiled-coil structure. Parallel helices were revealed for the rod 2A and linker 2 regions. Coiled coil structure was identified as beginning ~12 amino acids downstream from the start of rod 2B [Nicolet et al. 2010]. The locations of parallel helices and coiled-coil structure agreed between spectroscopic and crystallographic methods [Hess et al. 2006; Nicolet et al. 2010]

Very little structural data has been experimentally determined for tektins. Analysis of tektin amino acid sequences usually predicts 4 heptad repeat sections: helix 1A and 1B separated from helix 2A and 2B by a non-helical linker of approximately 50aa [Amos 2008]. Within tektin amino acid sequences are several conserved cysteine residues located with an

approximate periodicity of 8nm [Norrander et al. 1996]. Extrapolations of the predictions of coiled-coil structure along with the locations of cysteine residues led to the hypothesis that the assembly of axonemes is the result of numerous interactions between tektin filaments and tubulin with a limited number of other proteins [Norrander et al. 1996].

We have validated the use of SDSL EPR to determine structure in native vimentin intermediate filaments, determinations which have been substantiated in some cases by x ray crystallography of vimentin fragments. In this report we show that a similar approach can be used in studying the structure of tektins, which have thus far resisted a crystallographic approach. The application of SDSL EPR to tektins should help advance our knowledge of tektins, and also permit assessment of structural interactions between tektins and other filamentous structures within the cilium.

Methods

Cloning of human tektin genes

As described by proteomics, genomics and nucleic acid sequencing studies, the sea urchin *S. purpuratus* (Sp) contains 3 flagellar tektin genes: tektin A, tektin B, and tektin C [Chen et al. 1993; Norrander et al. 1992; Norrander et al. 1996]. Mammalian genomes typically contain genes for 5 tektins [Amos 2008]. Mammalian tektin genes 4, 2, and 1 correspond to Sp tektin genes A, B and C, respectively [Amos 2008]. The DNA/protein sequences for human tektins were obtained from Genbank (Human tektin 1: accession NP444515.1, human tektin 2: accession Q9UIF3, human tektin 4: accession AAH21716). Protein sequences were reverse translated using an *E. coli* highly expressed gene codon frequency chart (<http://genomes.urv.es/OPTIMIZER/>). To facilitate thio-specific attachment of the spin label at targeted sites within the protein, the 6 native cysteine codons (TGT/TGC) of human tektin 1 were changed to serine (AGC). This cys-minus modified gene was used as the template for additional single-cysteine mutants of tektin 1. Human tektin 2 and 4 were synthesized as native, cysteine containing proteins. Gene synthesis was performed by breaking the *E. coli* optimized DNA sequence into roughly 100 nt sections with 20 nucleotide overlaps at each end, for primer mediated synthesis using Taq polymerase (Invitrogen, Carlsbad, CA). PCR amplification of the complete human tektin coding sequences was performed with primers introducing a Nde I site at the amino terminus and an Eco RI site in the carboxy terminus. PCR products were cloned into pCR2.1 using the Invitrogen Topo TA kit (Invitrogen, Carlsbad, CA). Several positive clones were identified, sequenced and the correct coding sequence verified (UC Davis sequencing facility). For expression in *E. coli*, the tektin coding sequence was excised from pCR2.1 using Nde I and EcoRI and cloned into similarly digested pT7-7 [Studier et al. 1990]. Positive clones were screened by PCR, and potential expression clones subjected to DNA sequencing to validate the reading frame and vector (UC Davis sequencing facility). Arabinose inducible *E. coli* BL21AI (Invitrogen) were used for expression similar to our methods for vimentin production [Aziz et al. 2012; Hess et al. 2013; Hess et al. 2005; Hess et al. 2006; Hess et al. 2004; Hess et al. 2002].

Recombinant protein expression

Tektin was highly expressed in *E. coli* and formed inclusion bodies. These were purified from *E. coli* cell pellets using lysozyme/DNase/RNase [Nagai and Thogersen 1987]. Inclusion bodies were dissolved in 10mM Tris pH 7.5, 1mM EDTA, 200mM NaCl, 8M urea. In preparation for chromatography, the solution was clarified by centrifugation (10 minutes at 15K rpm, in a Sorvall SS-34 rotor, 15°C) and filtration (0.2 µm filter (Thermo Scientific Nalgene 0.2 micron SFCA filter)). The resulting predominantly tektin containing solution was then chromatographed over a Superdex 200 gel filtration column attached to a GE Healthcare AKTA FPLC. Fractions were screened by SDS-PAGE and peak fractions pooled. Tektin was further purified by FPLC using a HiPrep 26/10 desalting column followed by ion exchange chromatography on a Source Q. Purified protein was stored at -80°C long term or -20°C short term.

Preparation of antibodies

Rabbit polyclonal antibodies (Abs) were generated by Antibodies Inc, Davis, CA. Briefly, 2 mgs of purified human tektin 1 in urea were dialyzed against 5mM Tris, pH 7.5. This was delivered to Antibodies Inc for mixing with adjuvant and immunization of 2 rabbits. After booster inoculations and testing of sera, the rabbits were euthanized and blood collected and processed. Preliminary testing by ELISA (at AI) showed a high titer. Use of the anti-tektin 1 antibody produced a vigorous reaction against human tektin 1 in western blots.

Western blotting

Purified tektin 1, 2 and 4 was electrophoresed in duplicate on a 10% SDS-PAG (Hoefer Minigel) using standard procedures. Proteins were transferred to nitrocellulose overnight using aqueous buffers in a Hoefer transfer apparatus. Blocking of the membrane was performed using TBS-tween containing 3% normal goat sera and non-fat dry milk (5%). The primary Ab was diluted 1:10,000 in blocker and incubated overnight. Following several (3 × 10 minutes) TBS-tween washes, the secondary Ab (HRP conjugated GxRb #401315, Cal Biochem, San Diego, CA), diluted 1:2000 with blocker and incubated for 2 hours. Following additional TBS-tween washes, the immune complexes were visualized with a Chemiluminescent detection system (WesternBright ECL, Advansta, Menlo Park, CA). Controls consisted of pre-immune rabbit serum preincubated with *E. coli* extracts.

Immunohistochemistry

A C57 black 6 mouse harvested for other purposes was the source of testes for immunohistochemistry (mice were euthanized by dry CO₂ inhalation, as approved by UCD IAUCUC #17903). Testes were fixed by freeze substitution as described [Sun et al. 2015]. Fixed testes were embedded in paraffin, sectioned at 4 microns, mounted on slides, deparaffinized, and processed for immunofluorescence as described [Sun et al. 2015].

Assembly of tektin filaments/Electron microscopy

To promote assembly of tektin filaments, recombinant tektin protein in 8M urea buffers was dialyzed using regenerated cellulose dialysis tubing (10kD cutoff) (Thermo Fisher Scientific Products, Waltham, MA). Samples of ~ 100 µl with a protein concentration of 0.5-1.0 mg/ml

were dialyzed overnight against 5mM Tris, pH 7.5, with one buffer change in the morning followed by an additional 2 hour incubation. Samples were harvested by inverting the open end of dialysis tubing in an eppendorf tube and centrifuging the bag for 1-3 seconds. Ten microliters of the recovered sample were applied to carbon and formvar coated copper grids (Ted Pella, Redding, CA) using a pipet tip that had been cut to produce a wide bore. Grids were stained with 2% uranyl acetate for a few seconds, and excess UA removed by wicking. Samples were viewed in a Philips electron microscope with 80kV electron acceleration and 33Kx magnification [Hess et al. 2002].

Tektin filament samples for high resolution EM analysis were stained with 1% uranyl formate and visualized with a JEOL-1230 at 100kV electron acceleration; images were captured with a 2k Tietz CCD camera. Tilt series was collected on JEOL 2100F at $\times 50k$ magnification. The tilt angle was set from $+50^\circ$ to -50° with 1.5° increment. 3-D reconstruction was done using IMOD software [Kremer et al. 1996].

Circular dichroism spectroscopy

Circular dichroism spectroscopy (CD) measurements were performed on a Jasco J-715 spectropolarimeter equipped with a Peltier temperature control (Quantum Northwest) set to 25°C . For spectral acquisition, a tektin protofilament sample of 0.1 mg/ml in 5 mM Tris, pH 7.5 was placed in a 1 mm quartz cuvette and CD spectra were collected by signal averaging two scans in the region 190 to 260 nm using a scan speed of 20 nm/min, bandwidth of 1 nm and response time of 4 sec. Prior to analysis, all spectra were baseline-subtracted from the background buffer. The percent of secondary structure was estimated by deconvolution using the CAPITO CD analysis program [Wiedemann et al. 2013], which can be accessed on line at <http://capito.nmr.leibniz-fl.de>.

Preparation of mutants for spin-labeling and EPR analysis

The expression construct for human tektin 1 was created without endogenous cysteines. Thus, for SDSL-EPR, all that was needed was to introduce a cysteine codon followed by production of protein and spin labeling. Individual cysteine mutants (at positions 81-87) were constructed by Quik Change methodology (Bio Rad, Hercules, CA) using overlapping, double stranded, mutagenic primers purchased from Invitrogen. Mutants were DNA sequenced for verification of intended mutation.

Purified single cysteine containing proteins in chromatography buffer (with 8M urea) were incubated in 100 micromolar TCEP (tris-(2-carboxyethyl)phosphine, hydrochloride, Molecular Probes, Eugene, OR), followed by spin labeling with 500 micromolar O-87500 ((1-oxyl-2,2,5,5-tetramethyl-3-pyrroline-3-methyl) methanethiosulfonate-d15 [MTSL-d15] Toronto Research Chemicals, Toronto, Canada). The spin labeled protein was separated from unincorporated label by chromatography over a Source Q column. To assemble the protein into protofilaments [Grigoryan and Keating], the protein was then dialyzed against a low ionic strength buffer (5mM Tris, pH 7.5).

EPR measurements were carried out in a JEOL X-band spectrometer fitted with a loop-gap resonator [Hubbell et al. 1987]. An aliquot of the spin-labeled tektin protofilaments (5 μL) at a final concentration of ca. 50 μM protein was placed in a sealed quartz capillary and

inserted into the resonator. Spectra of samples at room temperature (20°-22° C) were obtained by a single 120 sec scan over a sweepwidth of 100G at a microwave power of 4 mW and a modulation amplitude optimized to the natural line width of 1G, as described previously [Chomiki et al. 2001] [Hess et al. 2004; Hess et al. 2002].

Results and Discussion

Expression of tektin and tektin 1 antibody

Using codons for E. coli highly expressed proteins, vectors for bacterial expression of human tektin 1, 2 and 4 were constructed; expression was robust, resulting in the formation of inclusion bodies. Purification of inclusion bodies yielded a highly tektin-enriched fraction. These were solubilized in a urea containing buffer and subject to gel filtration and ion exchange chromatography. Figure 1A shows aliquots of purified human tektin 1, 2 and 4 electrophoresed on an SDS-PAGE, stained with Coomassie blue.

Purified human tektin 1 was provided to Antibodies Incorporated (Davis, CA) for the production of rabbit polyclonal antibodies. Sera from both immunized rabbits reacted vigorously with tektin 1 on western blots. Western blot data show that the sera recognize human tektin 1, but not human tektin 2 or 4 (Figure 1B).

Previous reports have demonstrated the presence of tektins 1-5 in mouse sperm flagella [Cao et al. 2011]; structural studies to identify a tektin filament and/or the composition of such a filament in mouse or human have not been reported. An initial test of our anti-human tektin 1 sera on mouse testes revealed a pattern consistent with a flagellar location (Figure 1C). Alex-488 staining (Green) reveals short squiggles, indicative of flagella in profile, or puncta, indicating cross sectioning of flagella. DAPI Staining (Blue) of nuclei shows the round profile of a seminiferous tubule with green staining of spermatocyte/spermatozoa flagella inside.

Assembly of tektin filaments

Based on the successful assembly of IF proteins by dialysis from denaturing solutions, we applied the same approach to tektin. Initial experiments with various physiological buffers and salt concentrations resulted in the production of very small filaments and small aggregates of protein. In some cases, aggregates were large enough to pellet by centrifugation in a microfuge. In contrast to vimentin, human tektin 1 formed filaments most readily in low ionic strength Tris (Figure 2) and were progressively disassembled by increasing salt conditions (not shown).

Tektins, either individually or in all possible equimolar mixtures, were assayed for filament assembly. The best assembly was produced by human tektin 1 alone, resulting in long thin filaments. Despite these unsuccessful results with human tektin 2 and 4, our assembly of human tektin 1 is the first published report of successful *in vitro* assembly of any tektin.

Comparisons of our *in vitro* assembly of human tektins to native tektin structure is not straightforward. A number of tektin isoforms in human and mouse have been identified, and immunohistochemical data indicates the presence of tektins 1-5 in mouse sperm. But

whether all 5 tektin isoforms are present in the same filament or different filaments (in human or mouse) has not been determined. Indeed, immunohistochemical data from mice suggests different subcellular locations for different tektin isoforms [Larsson et al. 2000] [Iida et al. 2006; Matsuyama et al. 2005; Murayama et al. 2008].

However, the assembly properties of human tektin 1 can be viewed as somewhat consistent with what is known for sea urchin tektin assembly. Data from disassembled sperm flagella indicate that tektin C (homologue of human tektin 1) is crosslinked into homodimers [Setter et al. 2006]. The same experiments show that tektin A and B are crosslinked together into a heterodimer [Setter et al. 2006] [Pirner and Linck 1994]. Thus, assembly of human tektin 1 into a filament recapitulates the self-assembly property of sea urchin tektin C. With that being said, it is not clear if removal of tektin C from the tektin A-B-C containing filament removes an intact tektin C filament or tektin C monomers, dimers or oligomers. To our knowledge, neither purified sea urchin tektins nor recombinant sea urchin tektins have been assembled in vitro.

The assembly properties of human tektin 2 and 4 are more difficult to reconcile with sea urchin structure and assembly data. In sea urchin sperm flagella, the native tektin filament contains equimolar levels of tektin A, B, and C. Tektin C can be removed by washing the tektin filament with 4.5 M urea [Setter et al. 2006]. After tektin C extraction, tektin A and B remain assembled in a long, thin, filament. Because the filament formed by tektin A (human tektin 4) and tektin B (human tektin 2) is stable to different washes and purification steps, it would seem likely that human tektin 2 and 4 could be assembled into a similar heterodimeric filament. However, if this is possible, we have not identified the proper conditions.

Electron microscopy with tilt series data collection and automated reconstruction provides a higher resolution view of the tektin 1 filaments. In the higher magnification UF- stained sample, tektin 1 filaments appear as a sheet composed of distinct sub-filaments (Figure 2B). The filaments appear to wind around each other with a periodicity of 50nm. Arrowheads are placed to mark nodes where filaments cross. The estimate of 50nm per half turn is consistent with one full revolution of the filamentous coiling coinciding with the 96nm axonemal tubulin periodicity. The agreement of this value obtained with in vitro produced tektin filaments strongly suggests a relevant biological structure as this periodicity has been observed in both native tektin and in vitro assembled vimentin [Amos et al. 1986, Goldie et al. 2007].

Circular dichroism

In order evaluate the over-all helical content of the recombinant human tektin protein, protofilaments of human tektin 1 were analyzed by circular dichroism (CD). As shown in Figure 3, recombinant tektin 1 displays a CD spectrum indicative of a protein with high alpha helical content. Analysis of the spectrum by deconvolution predicts 78% alpha helical content. Furthermore, the 222 nm:208 nm intensity ratio is ~1.1, consistent with the helices in a coiled-coil arrangement [Zhou et al. 1992]. Our data are similar to a “preliminary analysis by circular dichroism spectroscopy” of a purified sea urchin tektin filament fraction [Linck and Langevin 1982]; these authors reported approximately 71% alpha helical content

for the filament fraction. Thus, CD data support the conclusion that recombinant tektin adopts a highly helical structure that is most likely the same as native tektin.

SDSL-EPR

We previously developed procedures for the use of SDSL-EPR to study the structure and assembly of the type III IF protein vimentin. During the performance of these studies, we showed that coiled-coil domains within vimentin produced an EPR pattern that conclusively identified the underlying heptad repeat pattern [Hess et al. 2005; Hess et al. 2004; Hess et al. 2002]. Each of these domains was subsequently crystallized and solved, confirming EPR results. This same methodology was used to demonstrate coiled-coil structure in kinesin [Acar et al. 2013].

With the ability to assemble tektin filaments, we began an SDSL-EPR investigation of tektin coiled-coil structure. Based on the long standing predictions and the recognizable heptad repeat pattern with hydrophobic *a,d* positions, the region 81-87 was chosen (the amino acid sequence and heptad repeat pattern are shown in Figure 4). To verify original predictions, we submitted the entire tektin amino acid sequence to *in silico* analysis with COILS software, (http://embnet.vital-it.ch/software/COILS_form.html). Regardless of the window size, COILS predicts positions 81-87 to be coiled coil.

The sequence of positions 81-87, LEQLVNV samples a full *a-g* heptad with hydrophobic and coiled coil permissive, leucines located at both *a* and *d* positions. Individual mutant proteins were produced, spin labeled and subject to dialysis. EPR spectra were collected as described. The resulting spectra were then normalized according to their integrated intensity (number of spins). The calculated spin number closely matched with the protein concentration for each sample (2.5 mg– 4 mg), indicating a similar labeling efficiency for each position. A similar and high labeling efficiency is expected since the samples were labeled under denaturing conditions. The normalized three-line (or three-peak) nitroxide EPR spectra are shown in Figure 4. Among the 3 nitroxide lines, the low-field peak best resolves multiple rates for motional averaging [Lopez et al. 2009], which can be characterized as strongly- and weakly-immobilized spin labels (see *s* and *w* designations in Figure 4). Remarkably, the EPR spectrum of each position within the 81-87 sequence displays a similar line shape consisting of well-defined strongly- and weakly-immobilized components. It should be noted that the (*w*) component is anisotropic and does not arise from free MTSL (unattached spin label), which is removed by chromatography followed by extensive dialysis. Although the fraction of the (*s*) and (*w*) components vary according to sequence position, the majority of side chains within each sample reside in the strongly immobilized (*s*) state, with a minor population in the more disordered (*w*) state. The observed two-component spectra can best be explained by the failure of a small fraction (on the order of 10% or less) of protein that does not fold or assemble properly, allowing the spin-labeled side chains to experience a faster correlation time. Thus the sharper *w* component most likely reflects protein that did not assemble properly, and the broader (*s*) component represents the predominant assembled protein fraction. Furthermore, the amplitude of the (*s*) component is substantial in each spectrum, suggesting the evaluated sites are similarly constrained in the assembled protein. As demonstrated previously, EPR

spectroscopy of site-directed spin labels can readily distinguish the interfacial *a,d* positions as their motion is sterically hindered relative to the other positions within the heptad repeat [Acar et al. 2013; Hess et al. 2006; Hess et al. 2004; Hess et al. 2002]. Thus the absence of distinct line shape changes as a function of sequence position argues against a parallel, in-register coiled-coil structure as exemplified in vimentin.

A representative coiled-coil spectra can be visualized using the example vimentin spectra provided in Figure 4. Spectra of a coiled-coil heptad would be constructed as follows: *a,d* like (position *a*), followed by 2 non *a,d* (positions *b* and *c*) followed by an *a,d* like spectra (position *d*) followed by 3 non *a,d* like spectra (positions *e, f, g*). The resulting series of spectra would look flatter and broader (positions *a* and *d*) mixed with taller and sharper (positions *b, c, e, f, g*). Tall peaks would be located at the *b, c, e, f, and g*, positions.

Spectroscopy clearly shows that alpha helical coiled-coil structure [Hess et al. 2006; Nicolet et al. 2010], not only generates differences in side chain mobility but also further broadening due to the magnetic interaction of apposing spin labels attached to the *a,d* positions in the dimeric structure. However, the spectra obtained from tektin shows no evidence of significant dipolar coupling at any of the seven residues measured. This observation indicates that if the tektin structure is based upon a dimer of in parallel, in register polypeptides, the side chains within the 81-87 region do not orient towards one another.

The EPR data we have obtained with tektin do not fit our established patterns for coiled-coil structure or the parallel helices structure of what was once termed rod 2A and linker 2 of vimentin. Within this region of vimentin, our characterization of 40 positions showed a recurring proximity and interaction between spin labels without exhibiting an *a,d* repeat pattern. We concluded that the protein structure was a parallel chains arrangement without coiled-coil consistent with conclusions from x-ray crystallography data [Nicolet et al. 2010]. Considering the EPR data from tektin positions 81-87, it is possible that this region is found in an out of register parallel chains structure, or perhaps an anti-parallel chain structure with rod 1A assembling with either of the other hypothesized rod domains.

The data presented clearly show that a range of experimental techniques previously applied to the study of Intermediate Filament structure and assembly could be brought to the study of tektin structure and assembly. *In vitro* production and purification of tektins 1, 2, and 4 is robust and assembly of human tektin 1 is possible. It is likely that tektins 3 and 5 would be similar. Whether assembly of different combinations of tektins 1-5 would be successful remains to be tested. However, our data show that analysis of multiple positions located in different hypothesized domains of tektin 1 by SDSL-EPR would lead to the determination individual domain structure and delineation of domains.

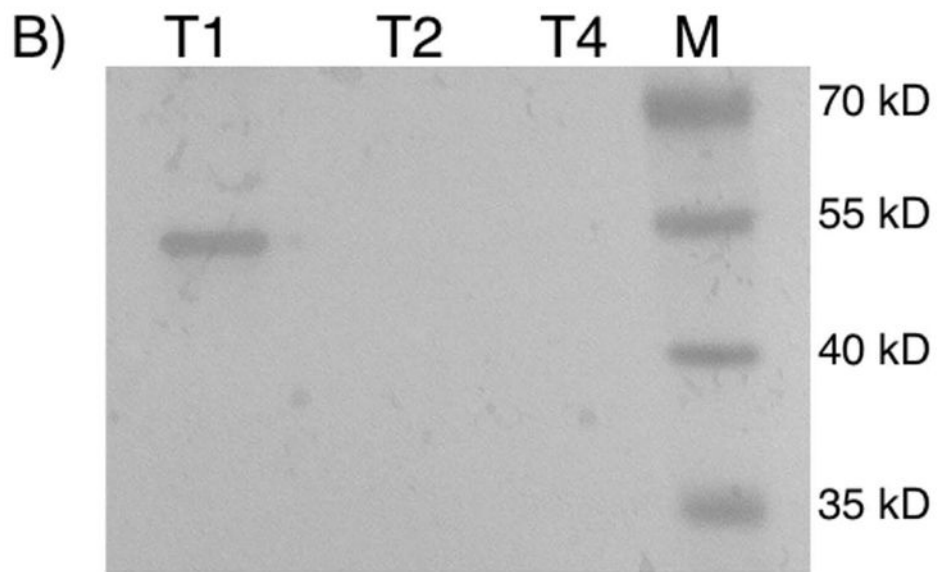
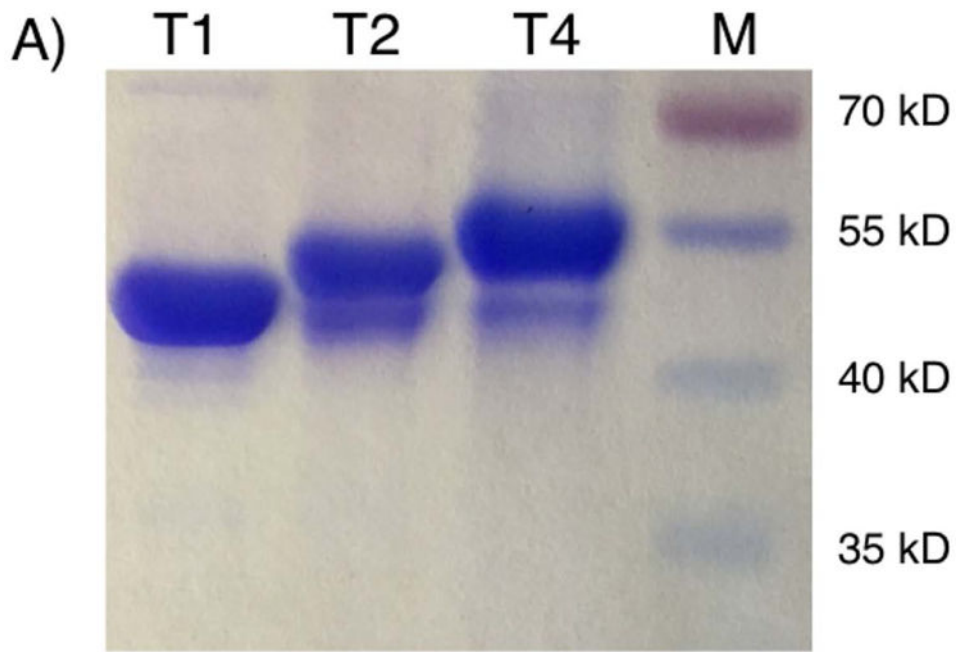
Acknowledgments

This work was supported by the following NIH grants: NEI EY015560 (to PGF) and NEI Core: P30 EY12576.

Literature cited

- Acar S, Carlson DB, Budamagunta MS, Yarov-Yarovoy V, Correia JJ, Ninonuevo MR, Jia W, Tao L, Leary JA, Voss JC, et al. The Bipolar Assembly Domain of the Mitotic Motor Kinesin-5. *Nature communications*. 2013; 4:1343.
- Amos LA. The Tektin Family of Microtubule-Stabilizing Proteins. *Genome biology Review*. 2008; 9(7):229.
- Amos WB, Amos LA, Linck RW. Studies of tektin filaments from flagellar microtubules by immunoelectron microscopy. *J Cell Sci*. 1986; (Suppl 5):55–68.
- Aziz A, Hess JF, Budamagunta MS, Voss JC, Kuzin AP, Huang YJ, Xiao R, Montelione GT, FitzGerald PG, Hunt JF. The Structure of Vimentin Linker 1 and Rod 1b Domains Characterized by Site-Directed Spin-Labeling Electron Paramagnetic Resonance (Sdsl-Epr) and X-Ray Crystallography. *J Biol Chem*. 2012; 287(34):28349–61. [PubMed: 22740688]
- Cao W, Ijiri TW, Huang AP, Gerton GL. Characterization of a Novel Tektin Member, Tekt5, in Mouse Sperm. *Journal of andrology*. 2011; 32(1):55–69. [PubMed: 20378928]
- Chang XJ, Piperno G. Cross-Reactivity of Antibodies Specific for Flagellar Tektin and Intermediate Filament Subunits. *The Journal of cell biology*. 1987; 104(6):1563–8. [PubMed: 2438286]
- Chen R, Perrone CA, Amos LA, Linck RW. Tektin B1 from Ciliary Microtubules: Primary Structure as Deduced from the Cdna Sequence and Comparison with Tektin A1. *Journal of cell science*. 1993; 106(Pt 3):909–18. [PubMed: 8308073]
- Chomiki N, Voss JC, Warden CH. Structure-Function Relationships in Ucp1, Ucp2 and Chimeras: Epr Analysis and Retinoic Acid Activation of Ucp2. *Eur J Biochem*. 2001; 268(4):903–13. [PubMed: 11179956]
- Crick FHC. The Packing of Alpha Helices: Simple Coiled Coils. *Acta Cryst*. 1953; 6:689–97.
- Ellenberger TE, Brandl CJ, Struhl K, Harrison SC. The Gcn4 Basic Region Leucine Zipper Binds DNA as a Dimer of Uninterrupted Alpha Helices: Crystal Structure of the Protein-DNA Complex. *Cell*. 1992; 71(7):1223–37. [PubMed: 1473154]
- Goldie KN, Wedig T, Mitra AK, Aebi U, Herrmann H, Hoenger A. Dissecting the 3-D structure of vimentin intermediate filaments by cryo-electron microscopy. *J Struct Biol*. 2007; 158:378–385. [PubMed: 17289402]
- Grigoryan G, Keating AE. Structural Specificity in Coiled-Coil Interactions. *Current opinion in structural biology*. 2008; 18(4):477–83. [PubMed: 18555680]
- Hess JF, Voss JC, FitzGerald PG. Real-Time Observation of Coiled-Coil Domains and Subunit Assembly in Intermediate Filaments. *J Biol Chem*. 2002; 277(38):35516–22. [PubMed: 12122019]
- Hess JF, Budamagunta MS, Voss JC, Fitzgerald PG. Structural Characterization of Human Vimentin Rod 1 and the Sequencing of Assembly Steps in Intermediate Filament Formation in Vitro Using Site-Directed Spin Labeling and Electron Paramagnetic Resonance. *J Biol Chem*. 2004; 279(43):44841–6. [PubMed: 15231822]
- Hess JF, Budamagunta MS, Fitzgerald PG, Voss JC. Characterization of Structural Changes in Vimentin Bearing an Epidermolysis Bullosa Simplex-Like Mutation Using Site-Directed Spin Labeling and Electron Paramagnetic Resonance. *J Biol Chem*. 2005; 280(3):2141–6. [PubMed: 15556930]
- Hess JF, Budamagunta MS, Shipman RL, FitzGerald PG, Voss JC. Characterization of the Linker 2 Region in Human Vimentin Using Site-Directed Spin Labeling and Electron Paramagnetic Resonance. *Biochemistry*. 2006; 45(39):11737–43. [PubMed: 17002274]
- Hess JF, Budamagunta MS, Aziz A, FitzGerald PG, Voss JC. Electron Paramagnetic Resonance Analysis of the Vimentin Tail Domain Reveals Points of Order in a Largely Disordered Region and Conformational Adaptation Upon Filament Assembly. *Protein Sci Research Support, NIH, Extramural*. 2013; 22(1):47–55.
- Hubbell WL, Froncisz W, Hyde JS. A Loop Gap Resonator. *Rev Sci Instrum*. 1987; 58:1879–86.
- Iida H, Honda Y, Matsuyama T, Shibata Y, Inai T. Tektin 4 Is Located on Outer Dense Fibers, Not Associated with Axonemal Tubulins of Flagella in Rodent Spermatozoa. *Molecular reproduction and development*. 2006; 73(7):929–36. [PubMed: 16596631]

- Knight PJ, Thirumurugan K, Xu Y, Wang F, Kalverda AP, Stafford WF 3rd, Sellers JR, Peckham M. The Predicted Coiled-Coil Domain of Myosin 10 Forms a Novel Elongated Domain That Lengthens the Head. *J Biol Chem.* 2005; 280(41):34702–8. [PubMed: 16030012]
- Konig P, Richmond TJ. The X-Ray Structure of the Gcn4-Bzip Bound to Atf/Creb Site DNA Shows the Complex Depends on DNA Flexibility. *J Mol Biol.* 1993; 233(1):139–54. [PubMed: 8377181]
- Kremer JR, Mastronarde DN, McIntosh JR. Computer Visualization of Three-Dimensional Image Data Using Imod. *Journal of structural biology.* 1996; 116(1):71–6. [PubMed: 8742726]
- Larsson M, Norrander J, Graslund S, Brundell E, Linck R, Stahl S, Hoog C. The Spatial and Temporal Expression of Tektin1, a Mouse Tektin C Homologue, During Spermatogenesis Suggest That It Is Involved in the Development of the Sperm Tail Basal Body and Axoneme. *European journal of cell biology.* 2000; 79(10):718–25. [PubMed: 11089920]
- Linck R, Fu X, Lin J, Ouch C, Scheffter A, Steffen W, Warren P, Nicastro D. Insights into the Structure and Function of Ciliary and Flagellar Doublet Microtubules: Tektins, Ca²⁺-Binding Proteins, and Stable Protofilaments. *The Journal of biological chemistry.* 2014; 289(25):17427–44. [PubMed: 24794867]
- Linck RW, Langevin GL. Structure and Chemical Composition of Insoluble Filamentous Components of Sperm Flagellar Microtubules. *Journal of cell science.* 1982; 58:1–22. [PubMed: 7183681]
- Linck RW, Chemes H, Albertini DF. The Axoneme: The Propulsive Engine of Spermatozoa and Cilia and Associated Ciliopathies Leading to Infertility. *Journal of assisted reproduction and genetics.* 2016; 33(2):141–56. [PubMed: 26825807]
- Lopez CJ, Fleissner MR, Guo Z, Kusnetzow AK, Hubbell WL. Osmolyte perturbation reveals conformational equilibria in spin-labeled proteins. *Protein Science.* 2009; 18(8):1637–52. [PubMed: 19585559]
- Matsuyama T, Honda Y, Doiguchi M, Iida H. Molecular Cloning of a New Member of Tektin Family, Tektin4, Located to the Flagella of Rat Spermatozoa. *Molecular reproduction and development.* 2005; 72(1):120–8. [PubMed: 15948161]
- Murayama E, Yamamoto E, Kaneko T, Shibata Y, Inai T, Iida H. Tektin5, a New Tektin Family Member, Is a Component of the Middle Piece of Flagella in Rat Spermatozoa. *Molecular reproduction and development.* 2008; 75(4):650–8. [PubMed: 17924527]
- Nagai K, Thogersen HC. Synthesis and Sequence-Specific Proteolysis of Hybrid Proteins Produced in *Escherichia Coli*. *Methods Enzymol.* 1987; 153:461–81. [PubMed: 3323806]
- Nicolet S, Herrmann H, Aebi U, Strelkov SV. Atomic Structure of Vimentin Coil 2. *Journal of Structural Biology Research Support, Non-US Gov't.* 2010; 170(2):369–76.
- Norrander JM, Amos LA, Linck RW. Primary Structure of Tektin A1: Comparison with Intermediate-Filament Proteins and a Model for Its Association with Tubulin. *Proceedings of the National Academy of Sciences of the United States of America.* 1992; 89(18):8567–71. [PubMed: 1528862]
- Norrander JM, Perrone CA, Amos LA, Linck RW. Structural Comparison of Tektins and Evidence for Their Determination of Complex Spacings in Flagellar Microtubules. *Journal of molecular biology.* 1996; 257(2):385–97. [PubMed: 8609631]
- O'Shea EK, Klemm JD, Kim PS, Alber T. X-Ray Structure of the Gcn4 Leucine Zipper, a Two-Stranded, Parallel Coiled Coil. *Science.* 1991; 254(5031):539–44. [PubMed: 1948029]
- Parry DA. Hendecad Repeat in Segment 2a and Linker L2 of Intermediate Filament Chains Implies the Possibility of a Right-Handed Coiled-Coil Structure. *J Struct Biol.* 2006; 155(2):370–4. [PubMed: 16713299]
- Pirner MA, Linck RW. Tektins Are Heterodimeric Polymers in Flagellar Microtubules with Axial Periodicities Matching the Tubulin Lattice. *The Journal of biological chemistry.* 1994; 269(50):31800–6. [PubMed: 7527396]
- Roy A, Lin YN, Agno JE, DeMayo FJ, Matzuk MM. Absence of Tektin 4 Causes Asthenozoospermia and Subfertility in Male Mice. *FASEB journal : official publication of the Federation of American Societies for Experimental Biology.* 2007; 21(4):1013–25. [PubMed: 17244819]
- Roy A, Lin YN, Agno JE, DeMayo FJ, Matzuk MM. Tektin 3 Is Required for Progressive Sperm Motility in Mice. *Molecular reproduction and development.* 2009; 76(5):453–9. [PubMed: 18951373]



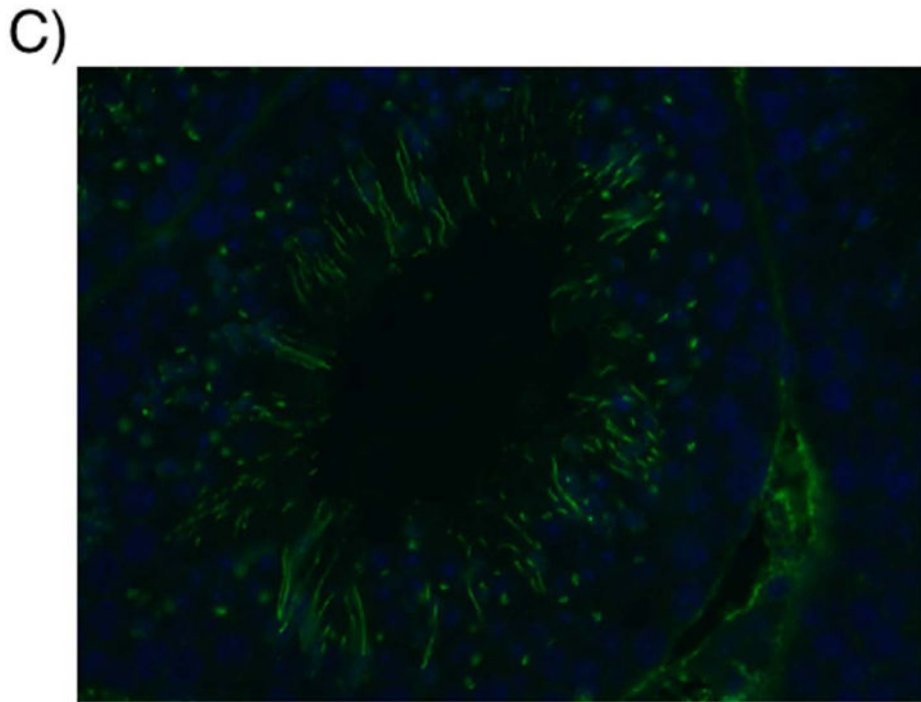
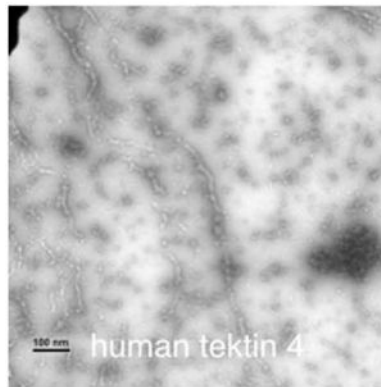
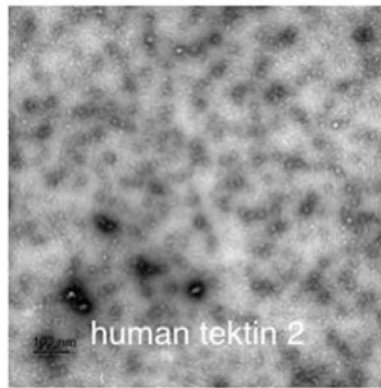
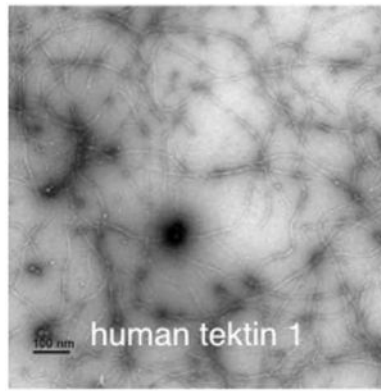


Figure 1. Coomassie stained SDS-PAGE of recombinant human tektins, western blot and antibody staining of mouse testes. A) approximately 10 μg of recombinant human tektin 1, 2, and 4 was electrophoresed on SDS-PAGE and stained with Coomassie blue. Size of standards is indicated along the right edge of the figure. B) Western blot of recombinant human tektins. Approximately 1 μg of each tektin was electrophoresed with an empty lane between samples (different loading pattern than in panel A). Following standard western blotting procedures, antibody reactivity was visualized by detection of chemiluminescent signal. C) Staining of mouse testes by rabbit anti-tektin 1 sera. Green indicates the location of the secondary antibody Alexa-488 staining. Blue is Hoescht nuclear stain.



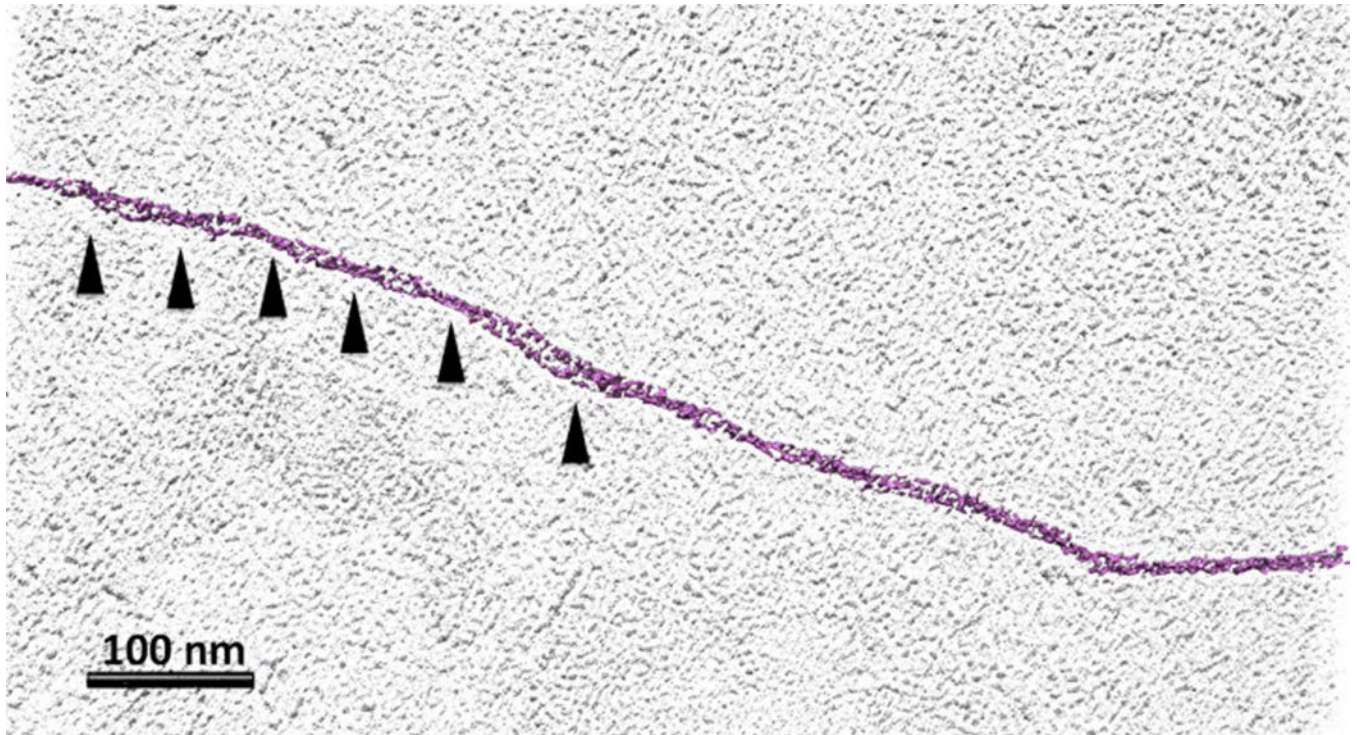


Figure 2.

A) Assembly of recombinant human tektins. Recombinant human tektin 1 (top), 2 (middle), and 4 (bottom). Tektin samples (~0.5 mg/ml) were dialysed against 5mM Tris pH 7.5 overnight with one buffer change. Filaments in tektin 1 are routine; tektin 2 and 4 have never produced similar filaments. Panel of tektin 4 represents the best assembly we have obtained for tektin 4. Scale bar in each panel indicates 100 μ m. B) 3-D electron tomographic reconstruction of 1% UF negatively stained tektin filament (magenta). Arrowheads indicate positions of subfilament unwinding/crossing over with a spacing of 50nm equivalent to period of approximately 100 nm. Scale bar=100 nm.

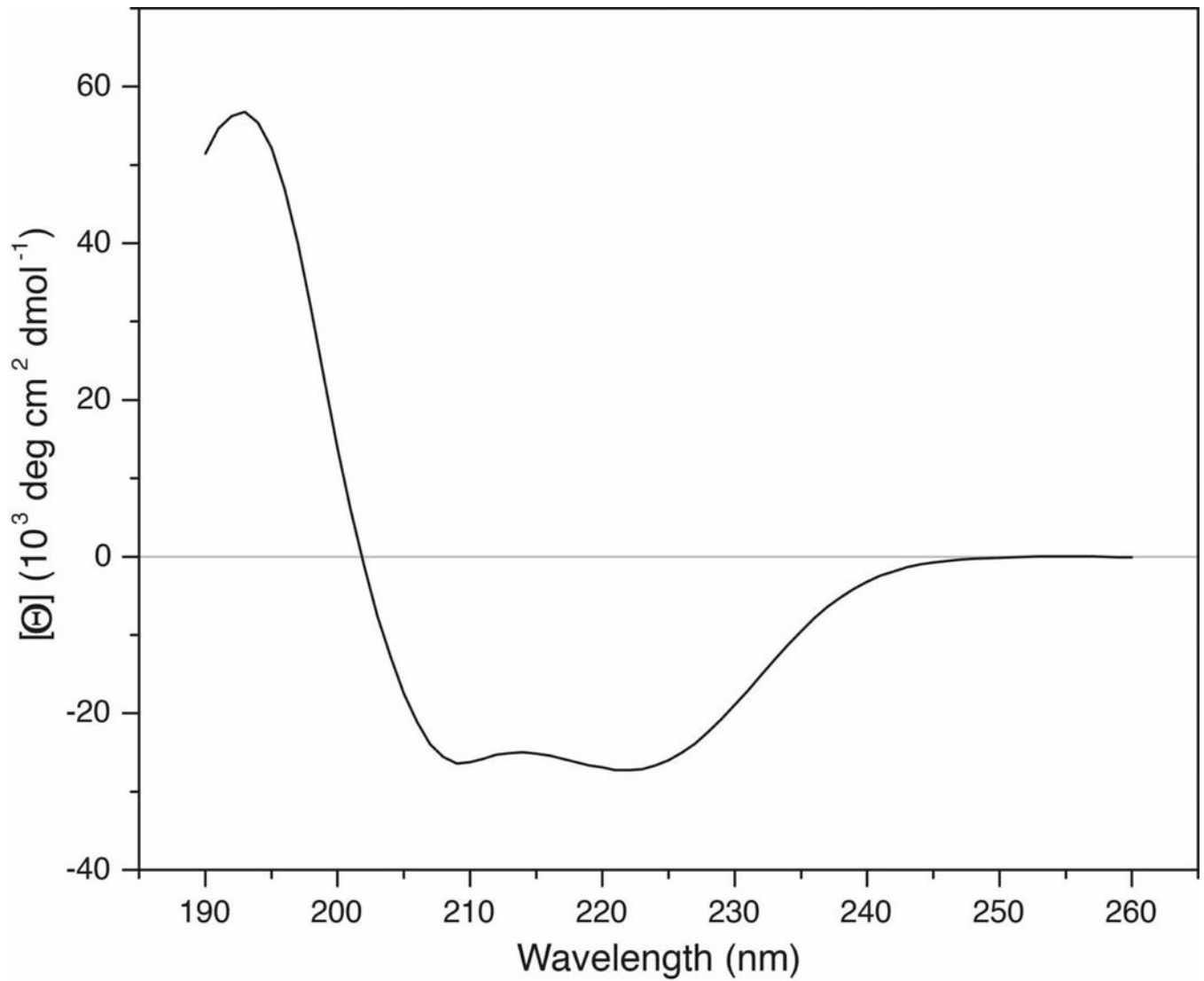


Figure 3.
The CD spectrum of tektin. Shown is the spectrum of human tektin 1 protofilaments (0.1 mg/ml) in 5 mM Tris, pH 7.5.

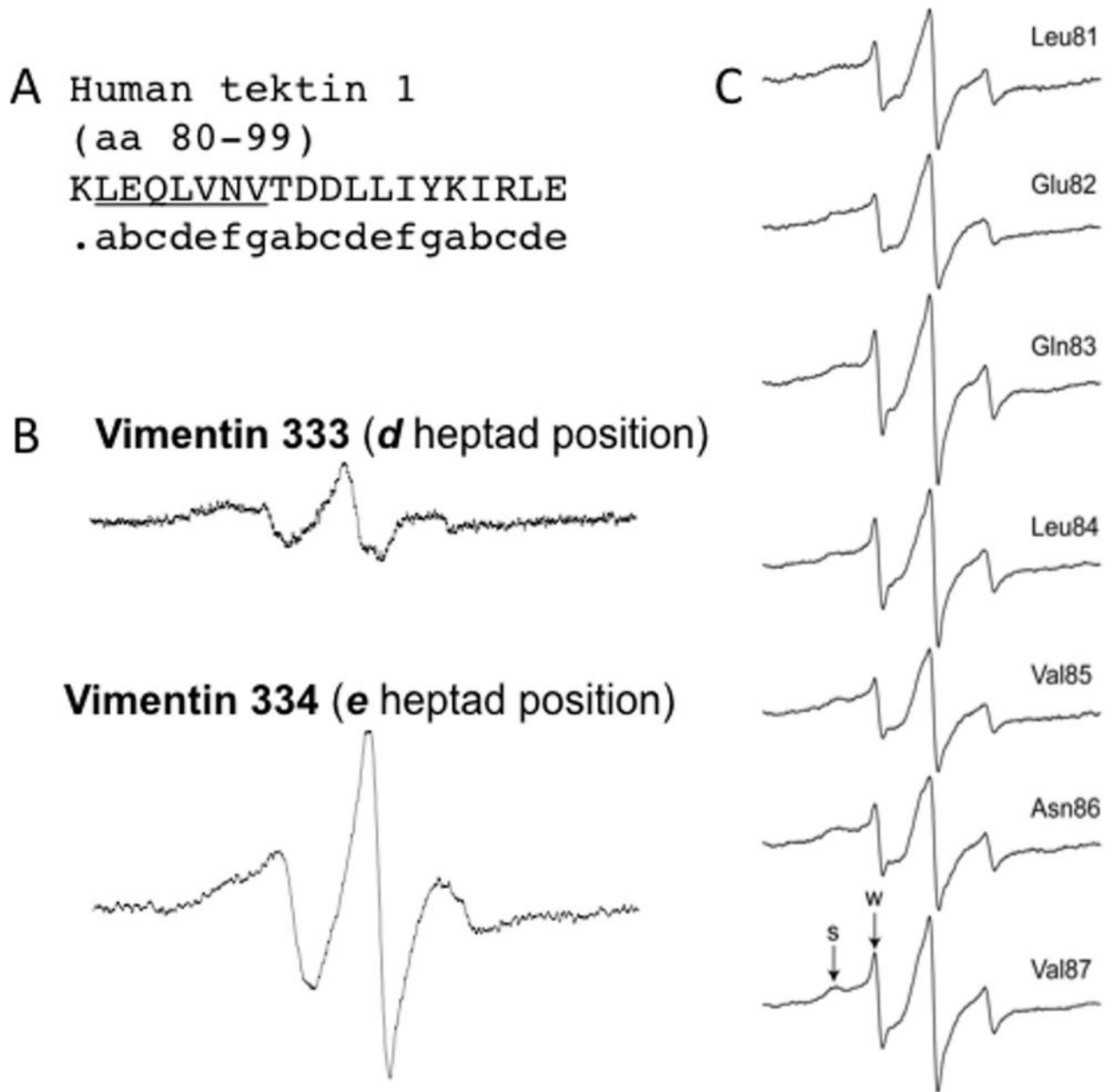


Figure 4. SDSL-EPR analysis of human tektin 1 positions 81-87

A) The amino acid sequence and heptad repeat pattern of human tektin 1, positions 80-99; positions 81-87 are underlined. The full heptad repeat pattern is written below the one letter amino acid code. B) Representative spectra from previously published vimentin experiments. Vimentin position 333 is a *d* heptad position; position 334 is an *e* heptad position. C) Normalized EPR spectra from human tektin 1 positions 81-87. At each position indicated, the wildtype amino acid has been replaced by cysteine and a spin label for collection of spectra. As discussed in the text, weak (w) and strong (s) components of the spectra, which are best resolved in the low field peak, are indicated.